Microgravity Sci. Technol.
DOI 10.1007/s12217-017-9543-z

ORIGINAL ARTICLE

Chronoamperometric Study of Ammonia Oxidation in a Direct Ammonia Alkaline Fuel Cell under the Influence of Microgravity

Raul Acevedo[1] · Carlos M. Poventud-Estrada[1] · Camila Morales-Navas[2] · Roberto A. Martínez-Rodríguez[2] · Edwin Ortiz-Quiles[2] · Francisco J. Vidal-Iglesias[3] · José Sollá-Gullón[3] · Eduardo Nicolau[2] · Juan M. Feliu[3] · Luis Echegoyen[4] · Carlos R. Cabrera[2]

Received: 19 May 2016 / Accepted: 6 March 2017
© Springer Science+Business Media Dordrecht 2017

Abstract This is a study of the chronoamperometric performance of the electrochemical oxidation of ammonia in an alkaline fuel cell for space applications. Under microgravity the performance of a fuel cell is diminished by the absence of buoyancy since nitrogen gas is produced. The following catalysts were studied: platinum nanocubes of ca. 10nm, platinum nanocubes on carbon Vulcan™ and platinum on carbon nanoonion support of ca. 10nm. These nanomaterials were studied in order to search for catalysts that may reduce or counter the loss of ammonia oxidation current densities performance under microgravity conditions. Chronoamperometries at potential values ranging from 0.2 V to 1.2V vs. cathode potential (breathing Air/300ml/min/82737 Pa) in 1.0 M NH_4OH (30ml/min in anode) were done during over 30 parabolas in NASA's C9 airplane The Weightless Wonder in January 2016 from Ellington Field Houston. The current densities at 15s in the chronoamperometry experiments showed diminishing values under microgravity and in some cases improvements of up to 92%, for Pt-carbon nanoonions, and over 70% for the three catalysts versus ground at potentials ranging from 0.2 to 0.4V after 5 minutes of chronoamperometric conditions. At higher potentials, 1.0V or higher, Pt nanocubes and Pt-carbon nanoonions showed enhancements of up to 32% and 24%, respectively. At these higher potentials we will have a contribution of oxygen evolution. The changes in current behavior are attributed to the sizes of the catalyst materials and the time needed for the N_2 bubbles detachment from the Pt surface under microgravity conditions.

Keywords Ammonia oxidation · Bubble · Platinum nanoparticles · Microgravity · Carbon nanoonions

Introduction

Fuel cells have been previously researched for various applications: proton electrode membrane fuel cells (Radenahmad et al. 2016), microbial fuel cells (de Vet and Rutgers 2007; Kannan and Kumar 2016), and alkaline fuel cells (Bayer et al. 2016) and have been used successfully in space applications since the Apollo missions (Warshay and Prokopius 1989). Hydrogen and methanol are commonly used in fuel cells.

Ammonia for fuel cells is cheap, its output produces water and nitrogen (clean fuel) and it is manufactured and stored on an industrial scale (Radenahmad et al. 2016; Erisman et al. 2008; Afif et al. 2016). Ammonia fuel cells have been proposed in a two-step process where the ammonia first is cracked into hydrogen and then used in a fuel cell (Cheddie 2012).

However, ammonia can be used as a fuel in a direct ammonia alkaline fuel cells, without the cracking step. The

✉ Carlos R. Cabrera
carlos.cabrera2@upr.edu

[1] Department of Physics, University of Puerto Rico, San Juan, Rio Piedras, 00931, Puerto Rico

[2] Department of Chemistry, University of Puerto Rico, San Juan, Rio Piedras, 00931, Puerto Rico

[3] Institute of Electrochemistry, University of Alicante, E-03080, Alicante, Spain

[4] Department of Chemistry, University of Texas at El Paso, El Paso, Texas, 79968-8807, USA

Published online: 13 April 2017

most accepted mechanism for the oxidation of ammonia was presented by Gerischer and Mauerer (1970):

$$NH_{3(aq)} \rightarrow NH_{3,ads} \quad (1)$$

$$NH_{3,ads} + OH^- \rightarrow NH_{2,ads} + H_2O + e^- \quad (2)$$

$$NH_{2,ads} + OH^- \rightarrow NH_{ads} + H_2O + e^- \quad (3)$$

$$NH_{x,ads} + NH_{y,ads} \rightarrow N_2H_{x+y,ads} \quad (4)$$

$$N_2H_{x+y,ads} + (x+y)OH^- \rightarrow N_2 + (x+y)H_2O + (x+y)e^- \quad (5)$$

$$NH_{ads} + OH- \rightarrow N_{ads} + H_2O + e^- \quad (6)$$

As it can be seen in the mechanism, the electrochemical oxidation of ammonia produces nitrogen gas. On the ground, nitrogen gas floats away because of the buoyancy of the gas leaving a clean platinum catalyst surface making of the platinum surface available to oxidize more ammonia. In the case of the electrochemical oxidation of ammonia under the influence of microgravity, the nitrogen gas produced near the surface of the catalyst stays in the vicinity due to the lack of buoyancy. This was demonstrated by cyclic voltammetry under microgravity conditions by Nicolau et al. (2012), showing a decrease in the ammonia oxidation peak current.

Previous experiments in microgravity have studied the formation of bubbles. Bitlloch et al. (2015) performed an analysis of bubble dispersion in turbulent jets based on data from drop tower experiments (Bitlloch et al. 2015). Sonoyama studied the formation of methane from CCl_2F_2 at a Cu modified gas diffusion electrode (Sonoyama 2007). Under the microgravity, the current efficiency for methane formation (the final product) increased. Thompson et al. studied their formation in a microgravity drop tower observing that in the absence of gravity surface tension is a driving force for the bubble detachment (Thompson et al. 1980). In addition, Kaneko et al. showed a decrease of current density with the formation of bubbles in microgravity (Kaneko et al. 1993). Herman et al. studied the effects of an electrical field on the formation of bubbles on microgravity, showing that at higher electrical fields better detachment of the bubbles is obtained (Herman et al. 2002). Carrera et al. studied the detachment of bubbles from a plate orifice and a tube orifice, showing that the plate orifice, having more area, the bubbles anchor to the surrounding surface making the detachment more difficult (Carrera et al. 2006). Buyevich and Webbon performed a theoretical study on bubble formation under microgravity finding that differences in the injector geometry could increase the bubble detachment volume due to conditions of incomplete wetting because of broadening of the bubble base (Buyevich and Webbon 1996, 1997). Balasubramaniam observed that the migration of a bubble under microgravity is due to a thermal gradient on the system (Balasubramaniam et al. 1996).

The formation of H_2 and N_2 formation of bubbles in ground forces has been studied at Pt ultramicro- and nanoelectrodes (Fernandez et al. 2014; Chen et al. 2014; Yang et al. 2015; Chen et al. 2015). They studied the formation of electrochemically generated H_2 and N_2 bubbles and subsequent detachment. The bubble detachment from the Pt electrode surface takes ca. 1-2s. Here we found that changes in ammonia oxidation currents changed after ca. 5-10 seconds under most of the Pt catalyst materials studies under microgravity.

The objective of the experiment is to compare the ammonia oxidation capabilities of three different catalysts in microgravity and on the ground (see Fig. 1). The platinum nanocubes by design have a preferential crystalline (100) sites which has shown better performance than (100) and (111) sites, oxidizing ammonia. (ref de Roberto). By using nanocubes on a carbon support (Vulcan XC-72™) we want to observe how the performance of the nanocubes change compared to the pure nanocatalyst. It is expected that dispersing the nanocubes would improve its current density. The surface area available of the pure platinum nanocubes is reduced, when platinum nanocubes in the vicinity occlude each other when they agglomerate. Also the performance of the pure platinum nanocubes and the nanocubes in Vulcan™ will be compared with platinum on carbon nanooinions. Carbon nanoonions have a higher surface area compared to Vulcan™, >984.3 m^2/g for carbon nanooinions (Echegoyen et al. 2010) vs. 262 m^2/g for carbon Vulcan™. (Sigma Aldrich)

Experimental Methods

Catalysts

Catalysts were synthesized in the laboratory. In particular, platinum nanocubes were synthesized by the water in oil emulsion method presented by Martinez-Rodriguez et al. (2014a, b) (see Fig. 2). 11 g of Brij30 and 2.1 mL of chloroplatinic acid 0.1M were added to 38.29 g of n-heptane in a container and the mixture was well mixed. Brij30 is a nonionic surfactant used to disperse the chloroplatinic acid particles by steric stabilization. This step was followed by the addition of 0.079g of sodium borohydride to reduce the dispersed platinum precursor. The reaction took place for 20 minutes. After it was finished, acetone was added to induce the precipitation of the platinum nanocubes. Once precipitated the particles were rinsed with acetone, methanol and nanopure water. Cubic particles formation was induced by adding HCl during the reduction process (Martinez-Rodriguez et al. 2014a).

The method for making the platinum supported on Vulcan™ nanoparticles is as follows: platinum nanoparticles were reduced with sodium borohydride by the method

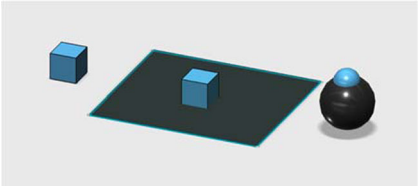

Fig. 1 Schematic representation of the three different nanomaterials used: Pt nanocubes, Pt nanocubes on Vulcan™ carbon and Pt nanoparticles on carbon nanoonions

previously explained, then added 39 mL of a solution of 5 mg/L of Vulcan™ in n-Heptane, to make a catalyst with a Pt/Vulcan™ ratio of 20:80. The solution was mixed for 30 minutes.

The platinum loading of the Pt in Vulcan™ catalysts was 20% Pt as determined by thermogravimetric analysis.

Platinum on carbon nano-onions were synthesized by the Rotating Disk Slurry Electrode (RoDSE) method presented by Santiago et al. (2012) (see Fig. 2b). Briefly, 50 mg of carbon nanoonions, produced from nanodiamond powder, were dissolved in 50 mL of 0.1 M sulphuric acid 0.1M and placed in the RoDSE electrochemical cell. A voltage of −0.2V vs. Ag/AgCl was applied to the glassy carbon rotating disk electrode while placed in the slurry solution. The rotating speed used was 900 rpm. While the potential was applied for 16 hours, 2 mL of 5 mM potassium hexachloroplatinate were added every two hours to the RoDSE electrochemical cell containing the carbon nanoonions in a slurry suspension. The produced platinum-carbon nanoonions catalyst slurry solution was vacuum filtered and dried in an oven at 60 °C for 12 hours. The platinum loading of the platinum on carbon nano-onion catalysts was 13% Pt as determined by thermogravimetric analysis.

Catalysts Ink Preparation

The following quantities were used for each catalyst ink preparation:

a. Pt nanocubes-5 mg of platinum nanocubes, 59 μL of FAA-3 liquid ionomer, 250 μL of dimethylformamide
b. Pt nanocubes-carbon Vulcan™- 25 mg, 59 μL of FAA-3 liquid ionomer, 750 μL of dimethylformamide
c. Pt carbon nanoonions-25 mg, 59 μL of FAA-3 liquid ionomer, 750 μL of dimethylformamide
d. Pt black-5 mg, 59 μL of FAA-3 liquid ionomer, 250 μL of dimethylformamide

To prepare the ink for each catalyst, 59 μL of FAA-3 liquid ionomer and 250 μL of dimethylformamide were dispensed into each vial containing the synthesized catalyst powders. The ink was homogenized in an ultrasonic bath for 2 hours. The catalyst ink was painted over the gas diffusion layer (GDL) on a hot plate at 60°C.

Membrane Electrode Assembly (MEA)

The Membrane Electrode Assembly (MEA) is the unit of the fuel cell that performs the electrochemical transformation of the fuel into electrical current. It consists of a Fumion ™FAA-3 PK-130 anion exchange membrane (Fumatech); on each side of the membrane there is a catalyst adhered to the membrane and an ELAT™LT1400W gas diffusion layer (Nuvant) over the catalyst. The microporous gas diffusion layer permits the evenly distribution of the fuel over the catalyst, the catalyst takes part into the oxidation and reduction reactions by lowering the activation energy for the reactions, and the proton conduction membrane transport the H^+ protons from the anode side to the cathode side. On the cathode side all MEAs had 1 mg/cm^2 of platinum black. The anode side carried three different catalysts: platinum nanocubes, platinum nanocubes on Vulcan™ support and platinum on carbon nanoonions support. The MEA is constructed by assembling one catalysts containing GDL against each side of the membrane. Care is taken to identify the anode side from the cathode side.

Fuel Cell

The experiment consists of a fuel cell with a 5 cm^2 active area (see Figs. 3 and 4). The fuel cell anode was fed with an ammonium hydroxide solution (1.0 M or 0.1 M) on a closed loop connected to a peristaltic pump at 30 ml/min. The cathode side was connected to a breathing air tank on the inlet and the outlet was connected to the exhaust system of the plane at 300 mL/min at 82737 Pa (Fig. 5).

Parabolic Flight

The microgravity experiments were performed aboard NASA's McDonnell Douglas C9 Skytrain II plane "The Weightless Wonder". The plane took off from Ellington Field Houston to perform a flight campaign in January 2016. The microgravity achieved by the parabolic maneuver was 0.02g for periods lasting 30 seconds.

Experiment Box

The experiment box was a modification of the box used by Nicolau et al. (2012). The box is a triple containment system made of Makrolon® designed and constructed for closed loop, self-contained experiments and it was modified to adapt an inlet hose from an external air tank and an outlet for the experiment exhaust to be connected to the

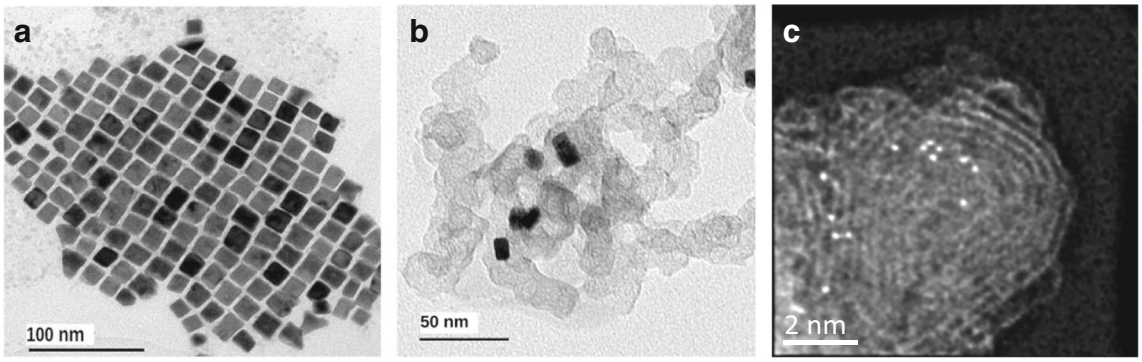

Fig. 2 Transmission electron microscopy of (**a**) Pt nanocubes, scale: 100 nm (Martinez-Rodriguez et al. 2014b), (**b**) Pt nanocubes on carbon Vulcan™, scale: 50 nm, and (**c**) Pt-carbon nanoonions, scale 2 nm, (Santiago et al. 2012)

plane exhaust system. The experiment box was bolted to the airplane floor.

Electronics Rack

The fuel cell was connected to a Biologic SP-50 potentiostat and a computer installed inside a rack system made with 80/20™ brand of structural framing system. The rack reside near the experiment box. The reference and counter electrode connections were on the cathode side of the fuel cell and the working electrode was connected to the anode.

Results and Discussion

The first experiment done with the fuel cell was to observe the current produced with respect to time at an applied potential to the anode vs. the cathode. The catalytic material used in the anode and the cathode of the fuel cell was a commercial product (1mg/cm^2 of unsupported 100% Pt Black, Sigma Aldrich). Figure 6 shows a transient representation of the current versus time for a fuel cell under an applied voltage of 0.45 V. The current was recorded for 10 parabolas during the microgravity and hypergravity period. It can be observed a decrease in current when the airplane

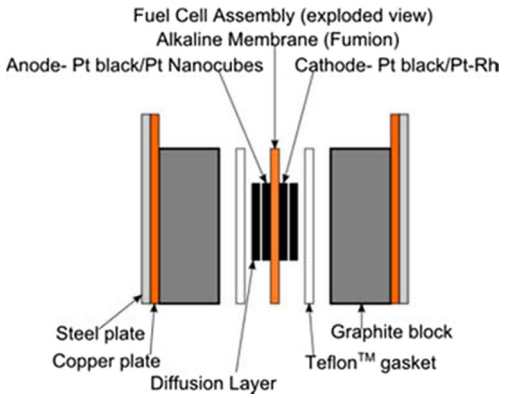

Fig. 3 Exploded side view of the direct ammonia alkaline fuel cell

change from hypergravity (410 μA at 1.7 g) to microgravity (370 μA at 0.02 g). This data validates the observations made in electrochemical half cells by Nicolau et al. (2012); there is an impairment of performance probably caused by the stagnant nitrogen gas, product of the oxidation of ammonia. On each cycle gravity changes from microgravity to normal gravity and then to hypergravity again. The current decrease phenomena are reversed when the plane returns to hypergravity, regaining the anode current production when the nitrogen gas floats away from the surface of the catalysts (Fig. 6).

Chronoamperometry with Platinum Nanocubes

The catalyst used in this experiment was pure platinum nanocubes produced in the laboratory. Platinum nanocubes are 10 nm in size and have crystalline (100) (110) and (111) sites. Figure 7s show chronoamperometric tests measuring the current produced by the fuel cell at different applied voltages (0.2 V, 0.4V, 0.6 V, 0.8V, 1.0V, and 1.2V vs. cathode). The anode had 0.1 M ammonia at 30 mL/min and on the cathode air at 300 mL/min. At 0.2 V and 0.6V, the current produced in microgravity is lower than that on ground conditions. On the other hand, the chronoamperometries at 0.4V show a very slight improvement of performance for the microgravity compared to the ground experiment up to a point where they stabilize over time giving the same performance as the ground case. This equalization of microgravity and ground performance occurs in the region of the graph where the concentration of ammonia in proximity to the electrode surface is depleted and then ammonia from the bulk solution diffuses toward the electrode. The current produced is a function of the concentration of ammonia, the concentration present is dependent on the diffusion mass transfer of ammonia from the bulk of the solution to the surface of the electrode. At 0.8V and 1.0V the performance at microgravity is better than that on the ground. Finally, at 1.2V the current performance on microgravity

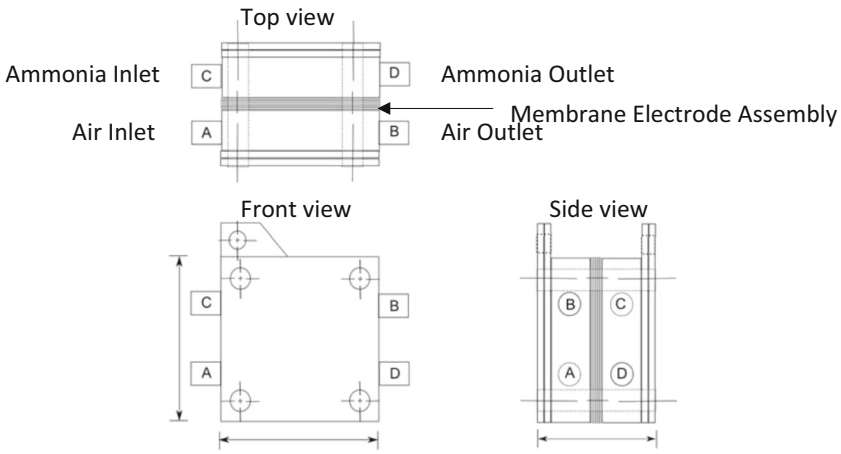

Fig. 4 Three side view of the fuel cell

is better during the period where the ammonia concentration near the electrode is not depleted, but once it enters the zone controlled by diffusion the performance decays and becomes lower than the ground counterpart. At this latter potential N_{ads}(adsorbed Nitrogen)is being formed which strongly adsorbs on platinum active sites, thus inactivating part of the platinum and reducing the catalyst activity in addition to the effect caused by the loss of buoyancy in microgravity.

Chronoamperometry with Platinum Nanocubes on Carbon Vulcan™

The catalyst material are the same platinum nanocubes used in the previous experiment dispersed on a carbon support with high surface area (Vulcan XC72™). The platinum nanocubes are 20% by weight of the catalyst. The nanocubes were deposited on the Vulcan™ by mixing the nanocubes and the Vulcan™ in acid. Figure 8 shows the chronoamperometric response of the fuel cell using platinum nanocubes supported on carbon Vulcan™ as anode at different applied potentials (0.2 V, 0.4V, 0.6 V, 0.8V, 1.0V and 1.2V). The anode is fed with 0.1 M ammonia solution at 30mL/min and the cathode with air at 300 mL/min.

At 0.2 V and 0.4V, the current produced in microgravity is significantly lower than that recorded on ground, while at 0.6 V and 0.8V, currents obtained in both conditions are very similar during the first 9 seconds of the experiments. After this time the microgravity current is slightly higher. On the contrary, for 1.0 V after this time the microgravity current becomes slightly lower than that on the ground. Finally, at 1.2V the microgravity current is lower than the current on the ground. Again, after 9 seconds is when the ammonia near the electrode is depleted and the current becomes diffusion controlled. The current produced is a function of the concentration of ammonia, the concentration present is dependent on the diffusion mass transfer of ammonia from the bulk of the solution to the surface of the electrode. As it is observed, the performance of the catalyst on microgravity improves with increasing values of applied voltage

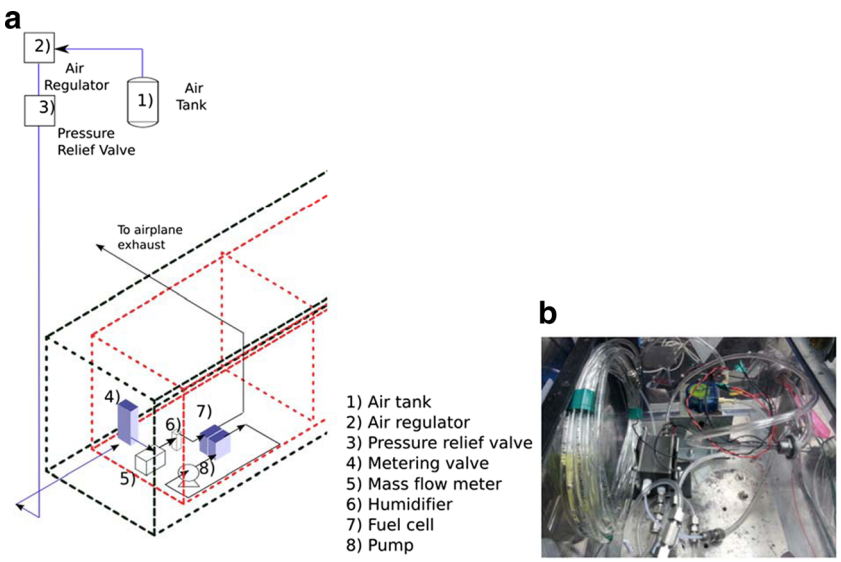

Fig. 5 Microgravity experiment set up. **a** schematic, **b** picture of the setup inside the experiment box

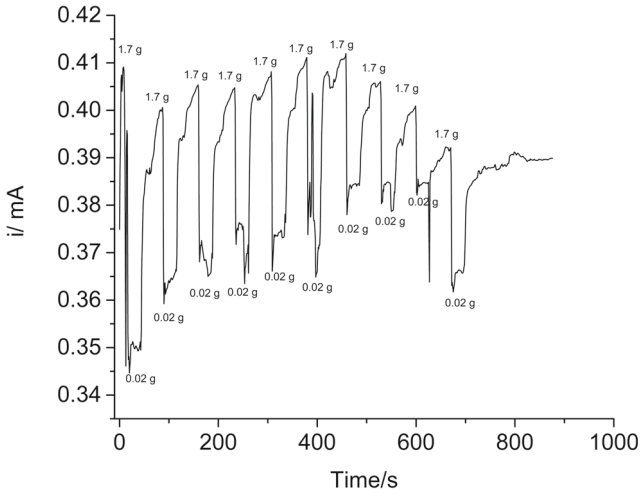

Fig. 6 Anode chronoamperometric data of an ammonia alkaline fuel cell at 0.45V vs. cathode (Breathing Air/300ml/min/82737 Pa) in 1.0M NH_4OH (30ml/min in anode) during 10 parabolas, from 0.02 g to 1.7 g. Anode (5mg of Pt black): NH_4OH 30ml/min, cathode (5mg of Pt black): Air 150 mL/min

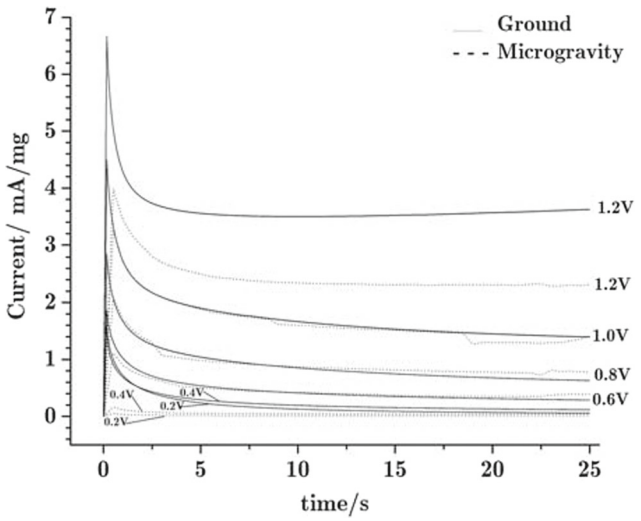

Fig. 8 Chronoamperommetry of ammonia oxidation at applied potentials of: 0.2, 0.4, 0.6, 0.8,1.0 and 1.2V vs. cathode (Breathing Air/300ml/min/82737 Pa) in 0.1M NH_4OH (30ml/min in anode). Anode-5.3mg of Pt-nanocubes in carbon Vulcan™ (ca. 20% metal loading) and cathode-5mg Pt Black

until it reaches 1.0 V, moment in which the microgravity current equates the current on ground and at even higher potentials (1.2V) then microgravity performance decreases in comparison with the ground experiments (Figs. 7 and 8).

Chronoamperometry with Platinum on Carbon Nanoonions

Platinum nanoparticles were electrodeposited on high surface area carbon nanoonions. Figure 9 show the chronoamperometric tests using platinum nanoparticles on carbon nanoonions as anode. The solution composition and flows as well as the applied potentials were the same as those measured for the other catalysts.

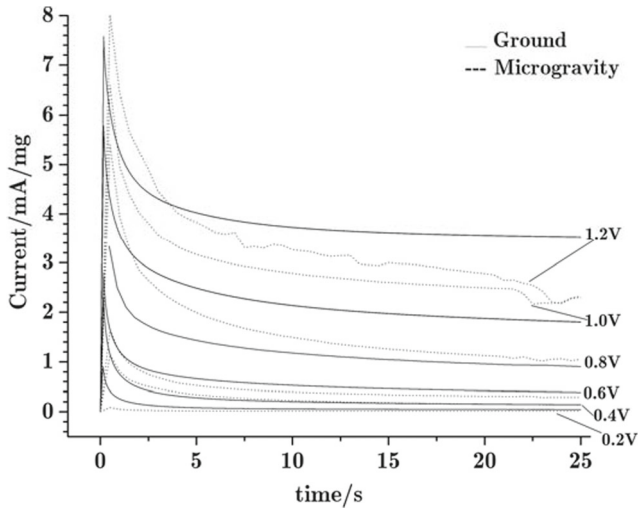

Fig. 7 Chronoamperommetry of ammonia oxidation at applied potentials of: 0.2, 0.4,0.6, 0.8,1.0 and 1.2V vs. cathode (breathing air/300ml/min/82737 Pa) in 0.1M NH_4OH (30ml/min in anode). Anode-5.2mg of Pt-nanocubes and cathode-5mg Pt Black

In this case, for the applied voltages of 0.2V, 0.6V and 0.8V the performance of the catalysts was reduced in microgravity conditions. On the other hand, at 0.4V, 1.0V and 1.2V the performance in microgravity decreased until after 5 to 6 seconds the current became diffusion controlled and the microgravity performance was better. The current produced is a function of the concentration of ammonia, the concentration present is dependent on the diffusion mass transfer of ammonia from the bulk of the solution to the surface of the electrode.

Comparative Performance of the Catalysts

Finally, in order to determine if there was a shift in the potential of the cathode electrode that was used as a counter/reference electrode, currents at 15s from the chronoamperometry were taken for each potential. A plot of currents at 15s vs. the applied potential is shown in Fig. 10.

Of all three catalysts, the platinum on carbon nanoonions showed the best performance increase in microgravity versus ground at 0.4V (99%). The high surface area and spherical morphology of the carbon nanoonions may be taking part on improving the release of the stagnant nitrogen gas that interferes with the oxidation of the ammonia. The higher surface area of the carbon nanoonions (>984.3 m^2/g vs. 262 m^2/g for carbon Vulcan ™) provides more nucleation sites where the nitrogen gas can grow and be released (Echegoyen et al. 2010). The improved current in

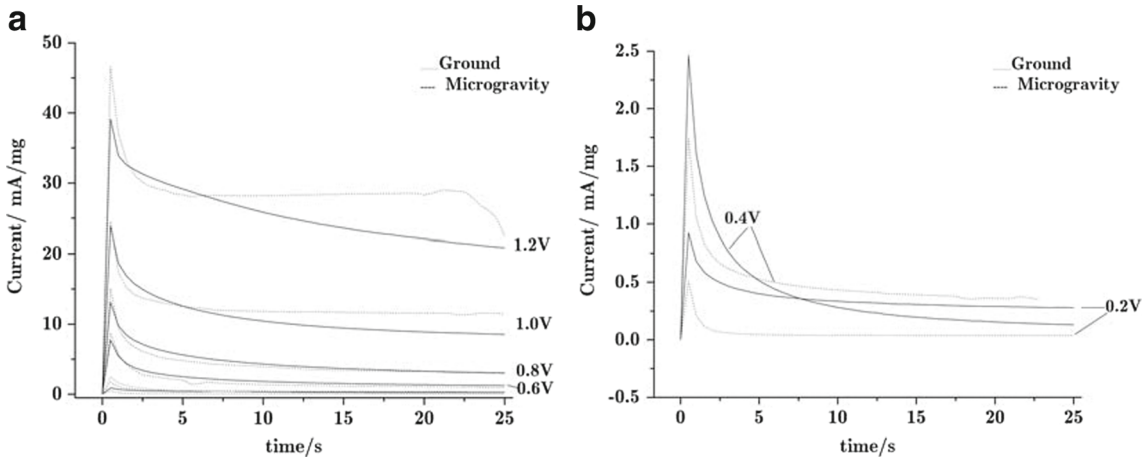

Fig. 9 **a** Chronoamperommetry of ammonia oxidation at applied potentials of: 0.2, 0.4, 0.6, 0.8, 1.0 and 1.2V vs. cathode (breathing Air/300ml/min/82737 Pa) in 1.0M NH4OH (30ml/min in anode). Anode- 3.2mg of Pt in carbon nanoonions (ca. 13% loading) and Cathode-5mg Pt. **b** expanded view of 0.2 V and 0.4 V

the platinum carbon nanoonions catalyst can be related to a better release of the nitrogen bubbles that hinder ammonia oxidation. The curved surface of the 5 nm nanoonion particles works in an analogous way to the tube orifice in Carrera et al. (2006) paper, in the sense that curvature offers less surrounding surface where the bubble can anchor (see Table 1).

Bubble Formation

The mechanism of bubble formation at ground has been studied at Pt ultramicroelectrodes and nanoelectrodes showing the formation of electrochemically generated H_2 and N_2 bubbles and subsequent detachment (Fernandez et al. 2014; Chen et al. 2014; Yang et al. 2015; Chen et al. 2015) The bubble detachment from the Pt electrode surface takes ca. 1-2s. In our case, we find that the detachment of N_2 from the platinum nanoparticles at microgravity conditions may be occurring at ca. 5-10 seconds in the time scale. This may be explained by the protective shielding the N_2 bubble may have on the Pt surface to avoid its prompt passivation that occurs in ground conditions. In general, under microgravity the lack of buoyancy in this nanomaterials have a positive effect on its catalytic performance at time longer that 5-10 seconds. This happens mainly at potentials higher than 0.8V vs. cathode. At such voltages it could be occurring an effect of electrowetting, the reduction of the surface tension and contact angle in the bubble caused by an electric field leading to bubble detachment from the electrode, it has been demonstrated experimentally the transport of air bubble in microchannels using this phenomenon (Zhao and Cho 2007).

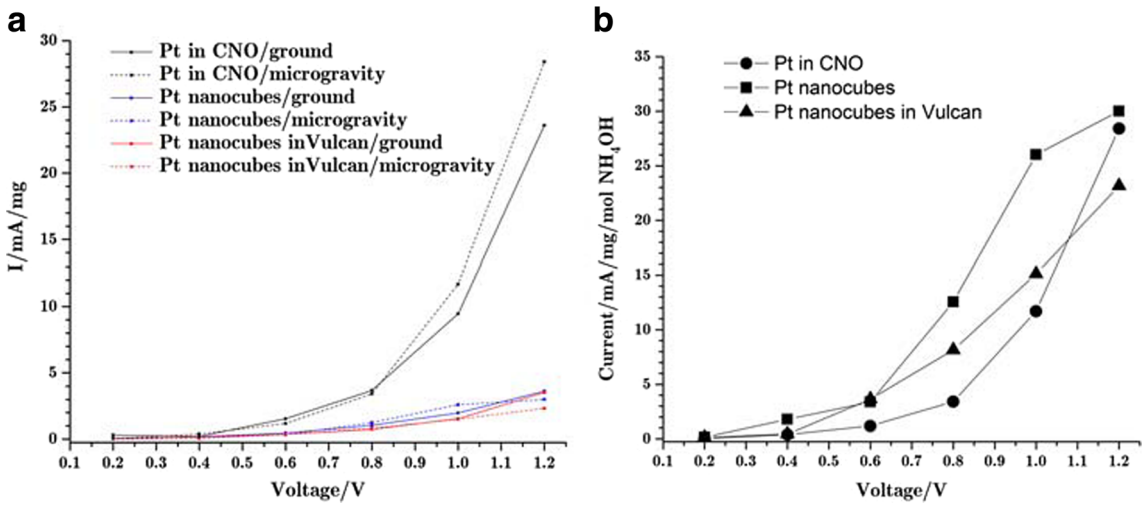

Fig. 10 (**a**) Current (normalized by Pt mass) values at 15 seconds obtained from the chronoamperometries performed at different potentials (from 0.2V to 1.2 V) shown in Figs. 5, 6, and 7 for Pt nanocubes, Pt nanocubes in Vulcan™ and Pt in carbon nanoonions and (**b**) Comparison of the currents normalized by Pt mass and molarity of NH_4OH for the three catalysts

Table 1 Comparative performance of catalyst in microgravity versus ground (positive values are an increase of performance) at 15s of the chronoamperometric data taken at 0.45V

Applied voltage vs. cathode (breathing air/300ml/min/82737 Pa) at in 0.1M NH_4OH (30ml/min in anode)	Pt nanocubes (100% metal loading)	Pt-nanocubes Carbon Vulcan ™ (20% metal loading)	Pt-nano-onions (13% metal loading)
0.2 V	−73%	−86%	−88%
0.4 V	5%	−71%	99%
0.6 V	−27%	3%	−23%
0.8 V	21%	9%	−7%
1.0 V	32%	−1%	24%
1.2 V	−17%	−34%	20%

The flight maneuver used was FL230-Fl310 so the experiment would observe a Δp between 43368.0 Pa and 55158.1 Pa, top to bottom of the parabola (the outside pressure being 40954.9 Pa and 28751.1 Pa). The cabin pressure does not excerpt direct influence in the fuel cell because the fuel cell was sealed in a double containment system. The vent system was sized, that in the event of a vent station being wide open, the flow rate was less than the make-up rate of the cabin pressurization system. Therefore, the vent does not affect significantly the cabin altitude.

The C9 plane's overboard vent system was connected to the outlet of the fuel cell cathode (air) side. The vent system could have created a pressure differential from the anode side to the cathode side. Considering that the trajectory of the plane is a parabola the pressure at the start of the parabola and at the end of the parabola would be quite similar, a difference would be noticed at the peak of the parabolic trajectory (ca. 12.5 s). No periodic or reversible effect was observed in the chronoamperometries, suggesting that the effect of the vent on the fuel cell current performance is negligible.

Conclusions

This research has shown the difference between the performance of the same catalysts in an ammonia fuel cell under microgravity and ground experimental conditions in terms of normalized current densities. In the case of a fuel cell with platinum black as catalyst on the anode there is a reduction in the produced mass-normalized current densities of around 7.5% between the hypergravity and microgravity experimental episodes. This decrease was shown to be reversed when gravity effects were once again applied to the fuel cell, confirming the direct influence from microgravity on the electrochemical oxidation of ammonia.

For the platinum nanocubes the decrease in current in microgravity was also shown, except for the applied voltages of 0.4V (5%), 0.8 V (21%) and 1.0V (32%), for which the current produced in microgravity was higher than on the ground. Nanocubes are 10 nm crystalline Pt (100) planes, being this orientation the most active for the ammonia oxidation.

For the platinum nanocubes supported on carbon Vulcan™, higher current densities were observed at 0.6V (3% current increase vs. ground) and 0.8V (9% current increase vs ground) in microgravity conditions when the ammonia electrooxidation was taking place at the diffusion controlled zone.

Finally, the platinum on carbon nanoonions support showed higher Pt mass-normalized current densities at 0.4V (99% current increase vs. ground), 1.0V (24% current increase vs. ground) and 1.2V (22% current increase vs. ground) in microgravity conditions.

Acknowledgements This work was financially supported by the NASA-MIRO Center for Advanced Nanoscale Materials at the University of Puerto Rico-Río Piedras Campus Grant number NNX10AQ17A and NASA-EPSCoR grant number NNX14AN18A, Puerto Rico NASA Space Grant Consortium: NASA cooperative agreement NNX10AM80H, NASA Flight Opportunities Program Announcement of Flight Opportunities (AFO) NOCT110 call #5 and Ministerio de Economía y Competitividad (projects CTQ2013-44083-P and CTQ2013-48280-C3-3-R). Also I want to say thanks to Robert Roe, Dominic Del Rosso and Terry Lee from the NASA Flight Opportunities Program, their support was immensely important to the success of this project.

References

Afif, A., Radenahmad, N., Cheok, Q., Shams, S., Kim, J.H., Azad, A.K.: Ammonia-fed fuel cells: a comprehensive review. Renew. Sust. Energ. Rev. **60**, 822–835 (2016). doi:10.1016/j.rser.2016.01.120

Balasubramaniam, R., Lacy, C.E., Woniak, G., Subramanian, R.S.: Thermocapillary migration of bubbles and drops at moderate values of the Marangoni number in reduced gravity. Phys. Fluids **8**(4), 872–880 (1996). doi:10.1063/1.868868

Bayer, T., Cunning, B.V., Selyanchyn, R., Daio, T., Nishihara, M., Fujikawa, S., Sasaki, K., Lyth, S.M.: Alkaline anion exchange membranes based on KOH-treated multilayer graphene oxide. J.

Membr. Sci. **508**, 51–61 (2016). doi:10.1016/j.memsci.2016.02.017

Bitlloch, P., Ruiz, X., Ramirez-Piscina, L., Casademunt, J.: Turbulent bubble jets in microgravity. Spatial dispersion and velocity fluctuations. Microgravity Sci. Technol. **27**(3), 207–220 (2015). doi:10.1007/s12217-015-9436-y

Buyevich, Y.A., Webbon, B.W.: Bubble formation at a submerged office in reduced gravity. Chem. Eng. Sci. **51**(21), 4843–4857 (1996). doi:10.1016/0009-2509(96)00323-5

Buyevich, Y.A., Webbon, B.W.: The isolated bubble regime in pool nucleate boiling. Int. J. Heat Mass Transfer **40**(2), 365–377 (1997). doi:10.1016/0017-9310(96)00097-x

Carrera, J., Parthasarathy, R.N., Gollahalli, S.R.: Bubble formation from a free-standing tube in microgravity. Chem. Eng. Sci. **61**(21), 7007–7018 (2006). doi:10.1016/j.ces.2006.07.021

Cheddie, D.: Ammonia as a hydrogen source for fuel cells: a review. In: Minic, D. (ed.) Hydrogen Energy - Challenges and Perspectives. InTech (2012)

Chen, Q., Luo, L., Faraji, H., Feldberg, S.W., White, H.S.: Electrochemical measurements of single h-2 nanobubble nucleation and stability at pt nanoelectrodes. J. Phys. Chem. Lett. **5**(20), 3539–3544 (2014). doi:10.1021/jz501898r

Chen, Q.J., Wiedenroth, H.S., German, S.R., White, H.S.: Electrochemical nucleation of stable n-2 nanobubbles at pt nanoelectrodes. J. Am. Chem. Soc. **137**(37), 12064–12069 (2015). doi:10.1021/jacs.5b07147

de Vet, S.J., Rutgers, R.: From waste to energy: First experimental Bacterial Fuel Cells onboard the International Space Station. Microgravity Sci. Technol. **19**(5-6), 225–229 (2007)

Echegoyen, L., Ortiz, A., Chaur, M.N., Palkar, A.J.: Carbon Nano Onions. In: Akasaka, T., Wudl, F., Nagase, S. (eds.) Chemistry of Nanocarbons. Wiley, Chichester (2010). doi:10.1002/9780470660188.ch19

Erisman, J.W., Sutton, M.A., Galloway, J., Klimont, Z., Winiwarter, W.: How a century of ammonia synthesis changed the world. Nat. Geosci. **1**(10), 636–639 (2008). doi:10.1038/ngeo325

Fernandez, D., Maurer, P., Martine, M., Coey, J.M.D., Moebius, M.E.: Bubble formation at a Gas-Evolving microelectrode. Langmuir **30**(43), 13065–13074 (2014). doi:10.1021/la500234r

Gerischer, H., Mauerer, A.: Untersuchungen Zur Anodischen Oxidation von Ammoniak an Platin-Elektroden. J. Electroanal. Chem. **25**(3), 421–433 (1970)

Herman, C., Iacona, E., Foldes, I.B., Suner, G., Milburn, C.: Experimental visualization of bubble formation from an orifice in microgravity in the presence of electric fields. Exp. Fluids **32**(3), 396–412 (2002). doi:10.1007/s003480100366

Kaneko, H., Tanaka, K., Iwasaki, A., Abe, Y., Negishi, A., Kamimoto, M.: Water electrolysis under microgravity condition by parabolic flight. Electrochim. Acta **38**(5), 729–733 (1993). doi:10.1016/0013-4686(93)80245-u

Kannan, M.V., Kumar, G.G.: Current status, key challenges and its solutions in the design and development of graphene based ORR catalysts for the microbial fuel cell applications. Biosens. Bioelectron. **77**, 1208–1220 (2016). doi:10.1016/j.bios.2015.10.018

Martinez-Rodriguez, R.A., Vidal-Iglesias, F.J., Solla-Gullon, J., Cabrera, C.R., Feliu, J.M.: Synthesis and Electrocatalytic Properties of h2SO4-induced (100) Pt Nanoparticles Prepared in Water-in-Oil Microemulsion. Chem. Phys. Chem. **15**(10), 1997–2001 (2014a). doi:10.1002/cphc.201400056

Martinez-Rodriguez, R.A., Vidal-Iglesias, F.J., Solla-Gullon, J., Cabrera, C.R., Feliu, J.M.: Synthesis of Pt Nanoparticles in Water-in-Oil Microemulsion: Effect of HCl on Their Surface Structure. J. Am. Chem. Soc. **136**(4), 1280–1283 (2014b). doi:10.1021/ja411939d

Nicolau, E., Poventud-Estrada, C.M., Arroyo, L., Fonseca, J., Flynn, M., Cabrera, C.R.: Microgravity effects on the electrochemical oxidation of ammonia: a parabolic flight experiment. Electrochim. Acta **75**, 88–93 (2012). doi:10.1016/j.electacta.2012.04.079

Radenahmad, N., Afif, A., Petra, P.I., Rahman, S.M.H., Eriksson, S.-G., Azad, A.K.: Proton-conducting electrolytes for direct methanol and direct urea fuel cells - a state-of-the-art review. Renew. Sust. Energ. Rev. **57**, 1347–1358 (2016). doi:10.1016/j.rser.2015.12.103

Santiago, D., Rodriguez-Calero, G.G., Palkar, A., Barraza-Jimenez, D., Galvan, D.H., Casillas, G., Mayoral, A., Jose-Yacaman, M., Echegoyen, L., Cabrera, C.R.: Platinum electrodeposition on unsupported carbon Nano-Onions. Langmuir **28**(49), 17202–17210 (2012). doi:10.1021/la3031396

Sonoyama, N.: Effect of micro gravity on the product selectivity of dichlorodifluoromethane electrolysis at metal supported gas diffusion electrodes. Microgravity Sci Technol. **19**(1), 22–24 (2007). doi:10.1007/bf02870985

Thompson, R.L., DeWitt, K.J., Labus, T.L.: Marangoni bubble motion phenomenon in zero gravity. Chem. Eng. Commun. **5**(5-6), 299–314 (1980). doi:10.1080/00986448008935971

Warshay, M., Prokopius, P.R.: The fuel cell in space: yesterday, today and tomorrow Retrieved from http://ntrs.nasa.gov/search.jsp?R=19900002488 (1989)

Yang, X., Karnbach, F., Uhlemann, M., Odenbach, S., Eckert, K.: Dynamics of single hydrogen bubbles at a platinum microelectrode. Langmuir **31**(29), 8184–8193 (2015). doi:10.1021/acs.langmuir.5b01825

Zhao, Y., Cho, S.K.: Micro air bubble manipulation by electrowetting on dielectric (EWOD): transporting, splitting, merging and eliminating of bubbles. Lab Chip. **7**(2), 273–280 (2007). doi:10.1039/B616845K